Mechanical Design of the Urban Air Mobility Side-by-Side Test Stand

Haley Cummings
Mechanical Engineer
NASA Ames Research Center
Moffett Field, California, USA

Gina Willink
Mechanical Engineer
NASA Ames Research Center
Moffett Field, California, USA

Christopher Silva
Aerospace Engineer
NASA Ames Research Center
Moffett Field, California, USA

ABSTRACT

The Urban Air Mobility Side-by-Side Test Stand (SBS) is a new capability for the National Aeronautics and Space Administration (NASA) to test the conceptual side-by-side rotorcraft configuration. This test stand enhances the experimental capabilities of the Revolutionary Vertical Lift Technology (RVLT) Project and is primarily designed to be tested in the U.S. Army's 7-by 10-Foot Wind Tunnel at NASA Ames Research Center. One of the goals for the SBS is to identify the optimal degree of rotor overlap that will yield the best aerodynamic performance. The SBS has two counter-rotating, intermeshing rotors that can vary in lateral separation. The test stand can pitch nose up and nose down, with each rotor having the capability to be trimmed independently through cyclic and collective controls. Six-axis load cells and rotary torque sensors are placed underneath each rotor to measure the thrust, torque, and side force from each rotor system. This paper describes the mechanical design of the SBS and outlines the structural analyses conducted to ensure a safety factor of 4 for ultimate strength and 3 for yield strength during all experimental testing.

INTRODUCTION

Many new concept vehicles with various rotor and wing configurations are emerging into the Urban Air Mobility (UAM) market faster than rigorous testing and analysis can be conducted. These vehicles are often marketed as personal flying vehicles or candidates for "flying taxis" [1]. Previously, little experimental data existed for these types of multirotor configurations. However, at the National Aeronautics and Space Administration's (NASA) Ames Research Center (ARC), there have been a few recent testing campaigns to investigate multirotor systems. In 2015 and 2017, two wind tunnel test campaigns were conducted in the U.S. Army's 7-by 10-Foot Wind Tunnel (7x10) of multirotor Unmanned Aerial System (UAS) vehicles and the aerodynamic performance of five off the shelf quadcopters was measured [2–4]. In 2019, the Multirotor Test Bed (MTB) was tested in the 7x10 and has begun to expand understanding of the complicated aerodynamics associated with multirotor systems [5–7]. Despite these experimental campaigns, there is still a dearth of analytical and experimental data to aid the public sector in the design of UAM vehicles.

NASA's Revolutionary Vertical Lift Technology (RVLT) Project is developing concept vehicles that can be utilized by the public sector to develop new, unique vehicles. NASA's concept vehicles are intended to combine various common aspects of the emerging concept vehicles and provide analytical and experimental data to aid the public sector in their design work. Some of the concept vehicles include a tiltrotor configuration, a quadrotor configuration, and a side-by-side configuration [1,8–12]. Analytical studies are ongoing for these configurations. The design and manufacture of test stands to experimentally validate the analytical analysis is also ongoing.

The side-by-side concept vehicle, seen in Figure 1, is one of the upcoming experimental campaigns. The vehicle features counter-rotating, intermeshing rotors that are supported by wings on either side of the aircraft. Previous research indicates that there is an optimal amount of overlap that the rotors should have to further improve aerodynamic performance [13–19]. Measuring the performance at various degrees of rotor overlap to analyze where the maximum performance occurs is one of the test objectives for NASA's side-by-side wind tunnel test campaign. This paper is intended to explore the mechanical design and analysis of the wind tunnel test stand for the UAM side-by-side concept vehicle configuration.

Figure 1: Conceptual Side-by-Side Aircraft [1]

Presented at the Vertical Flight Society's 9th Biennial Autonomous VTOL Technical Meeting, Virtual, January 26-28, 2021. This is a work of the U.S. Government and is not subjected to copyright protection in the U.S.

DESIGN

The Urban Air Mobility Side-by-Side Test Stand (SBS) consists of three main components: the gear box, the strongback, and the rotor head stack, as seen in Figure 2; note that there are two rotor head stacks due to the symmetry of the system. Throughout this paper in the figures of the SBS assembly, green components are custom design/machining, yellow components are commercial off-the-shelf, and blue components are sensors (torque sensor and load cell).

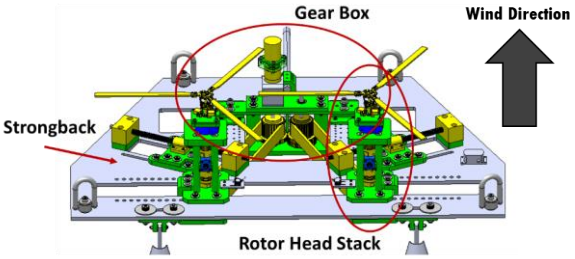

Figure 2: SBS with major components highlighted

The mechanical design goals for the SBS required that the stand incorporate two intermeshing, counter-rotating 14-inch radius rotors. These rotors needed to be able to change the lateral spacing such that the SBS could be tested with overlapping rotors as well as with the rotors completely separated. The maximum and minimum lateral spacing between the rotor centers is 45 inches and 23 inches respectively, shown in Figure 3. The mounting holes are spaced in 1-inch increments.

The rig was required to incorporate both collective and cyclic controls, which will be used to trim the rotors. Both collective and cyclic are controlled during testing from the control room. The SBS was designed to be tested in the U.S. Army's 7-by 10-Foot Wind Tunnel and connects to the test section via two front struts and one tail strut which are secured to the strongback. The tail strut of the 7x10 is outfitted with a linear actuator, which enables the SBS to pitch forward 5 degrees and backwards 10 degrees. This pitch mechanism is controlled from the control room during testing.

There is a JR3 six-axis load cell installed under each rotor and a Futek rotary torque sensor in line with each rotor shaft. The SBS is also outfitted with an RPM sensor on each rotor head stack as well as an accelerometer on the strongback which measures the pitch of the rig. Three off-the-shelf servos are incorporated on each rotor head stack.

The rotor head chosen for the test is the SAB Goblin 380 KSE (three-bladed) rotor head. This off-the-shelf rotor head includes a swashplate with collective and cyclic control. The blades used for the initial SBS test will be the SAB Goblin 380 carbon fiber blades.

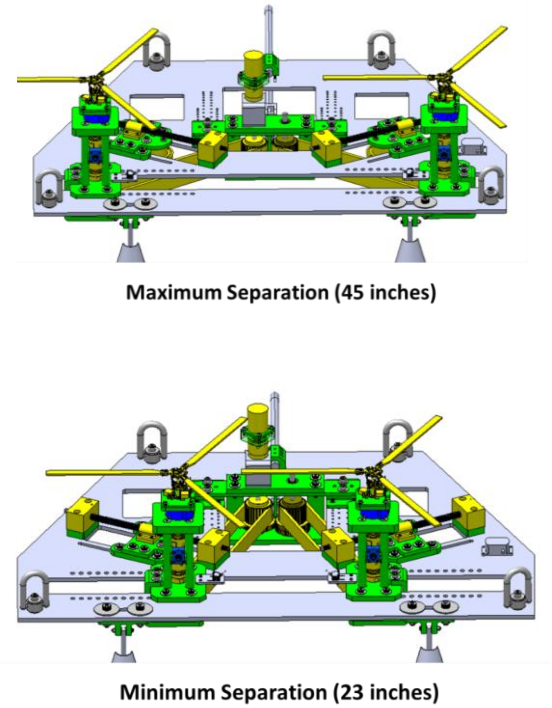

Figure 3: Maximum and minimum rotor separation for the SBS

The overall dimensions of the SBS are 61 inches from starboard to port, 40.75 inches from front to back (not including the shepherd's crook that attaches the SBS to the wind tunnel), and 15.85 inches from the bottom of the strongback to the top of the rotor head, as seen in Figure 4.

The SBS consists of several off-the-shelf components as well as custom designed and manufactured parts. The custom parts were machined primarily from Aluminum 6061-T6 and 17-4PH H900 Stainless Steel.

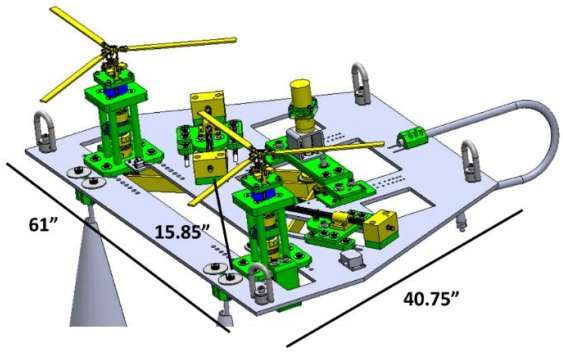

Figure 4: Overall dimensions of the SBS

The SBS was designed to withstand all planned testing conditions in the 7x10 with a significant safety margin, as well as be able to take accurate data measurements. NASA design guidelines were followed throughout the SBS design process, and mechanical and fabrication best practices were also followed, with guidance from the NASA Ames machine shop [20,21].

Gear Box

The motivation behind the gearbox design was to ensure that the rotors were properly synchronized to each other to reduce the possibility of the rotors interfering while they overlapped. Intermeshing rotors are less likely to fail if they are synced to one motor via gears and pulleys. In addition, it was desired to incorporate a rotary torque sensor in line with each rotor head stack, which made it impractical to use a direct drive motor in line with the rotor head stack. Thus, the rig was required to incorporate a mechanical coupling between the propulsion systems of each rotor. To achieve this, a single motor and Off-the-Shelf (OTS) gear box were used. This motor and OTS gear box combination drive two spur gears, which forces one of the rotors to be counter-rotating. Each shaft with a spur gear also includes a toothed pulley, which connects to a toothed belt and another toothed pulley on each rotor head stack. The motor, OTS gear box, two shafts, two spur gears, and two pulleys are constrained to a gear box housing, as seen in Figure 5.

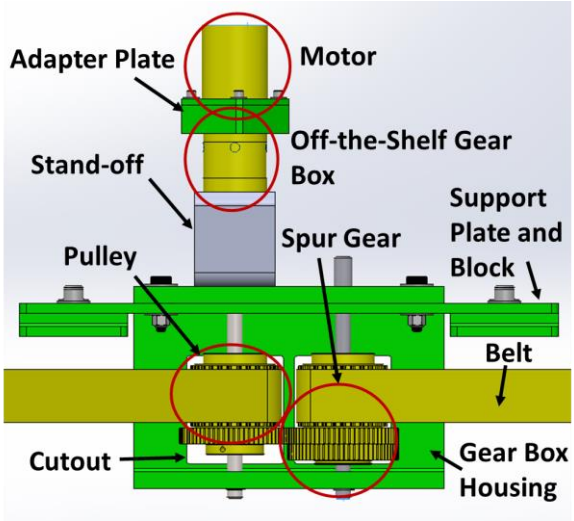

Figure 5: Gear box with major components labeled

The motor incorporated in the design is the Scorpion HKIV-5035-380KV brushless DC motor. The OTS gear box incorporated is the Neugart PLE060-005. From the bottom of the shafts to the top of the motor is 17.58 inches. The width of the gear box is 20 inches and the depth is 4 inches, as seen in Figure 6.

The two main machining methods that were considered for the gear box were bending and using a computer numerical control (CNC) machine to cut out the shape. However, due to the required flatness and parallelism because of the mounting of the off-the-shelf gear box and the shafts, the CNC method was chosen. This method takes longer and uses more material but results in higher machining accuracy. The cutouts in the back of the gear box were required because the material could not be found in a sufficient size to accommodate the entire radius of the spur gears. Thus, the cutouts were incorporated to avoid interference with the gears.

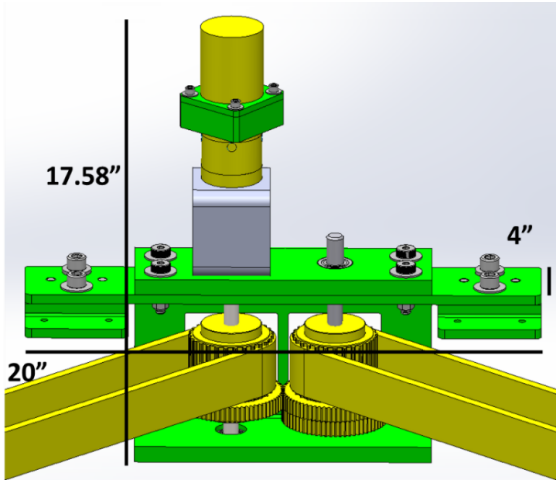

Figure 6: Overall dimensions of the gear box

The material chosen for the gear box was 17-4PH H900 Stainless Steel due to the material’s high strength and stiffness.

The gear box includes a stand-off, which ensures proper placement of the motor relative to the OTS gear box. The custom machined standoff is made of standard A500 steel tubing.

The Neugart OTS gear box was designed to mate with a NEMA standard motor. However, the Scorpion motor does not have NEMA standard mating parts. Thus, a motor/gear box adapter plate was designed and incorporated to attach the two together. The adapter plate assembly consists of two pieces that are bolted together to attach the Scorpion motor and the Neugart gear box, as seen in Figure 7. The adapter plate assembly was made from Aluminum 6061-T6 and was anodized.

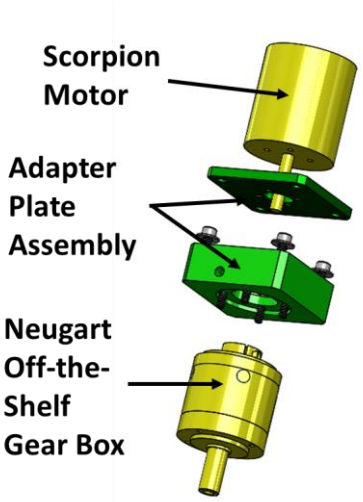

Figure 7: Motor, Off-the-Shelf gear box, and adapter plate assembly shown in an exploded view

The gear box is supported by a 17-4PH H900 plate which attaches to two blocks mounted on the strongback. The blocks are attached to the strongback by four 1/4-inch shoulder screws spaced in such a way that the blocks can be moved along the length of the strongback. This is done so that a minimal amount of tension is maintained on the belts when the lateral spacing of the rotors is adjusted. Most of the tension on the belts is applied through the use of a tensioner/idler pulley, described later in the paper.

Strongback

The strongback of the SBS is made of 17-4PH H900 Stainless Steel and is 1/2-inch thick. The strongback itself holds all of the other components of the SBS and attaches to the wind tunnel. The overall dimensions of the strongback are 61 inches wide by 40.75 inches long, as seen in Figure 8.

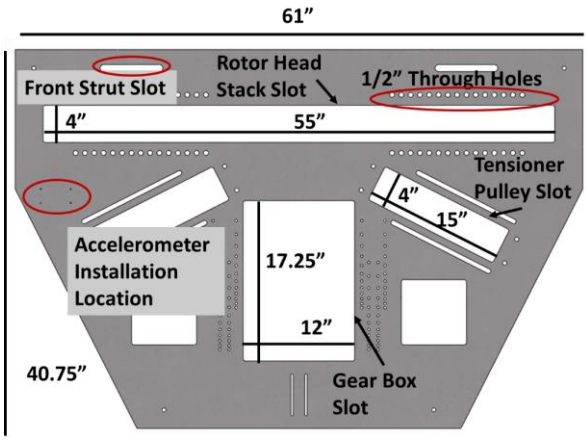

Figure 8: Top view of strongback

The strongback is secured to the 7x10 wind tunnel test section via two front struts and one tail strut. There are slots in the rear of the strongback which attach to the shepherd's crook and sting block assembly, as seen in Figure 9. This assembly was used in previous tests conducted in the 7x10 such as the High Efficiency Tilt Rotor (HETR) test. The sting block is attached to the strongback using six 1/4-inch shoulder screws through two slots. The slots were chosen instead of through holes because the placement of the tail strut in the 7x10 is variable. Thus, the slots allow for ease of assembly when attaching the SBS to the wind tunnel. The shepherd's crook is assembled to the sting block using two 1/4-inch dowel pins. The tail strut is attached to the clevis of the shepherd's crook using a 1/4-inch shoulder screw. As mentioned previously, the tail strut of the 7x10 includes a linear actuator which allows the SBS to pitch nose up and nose down.

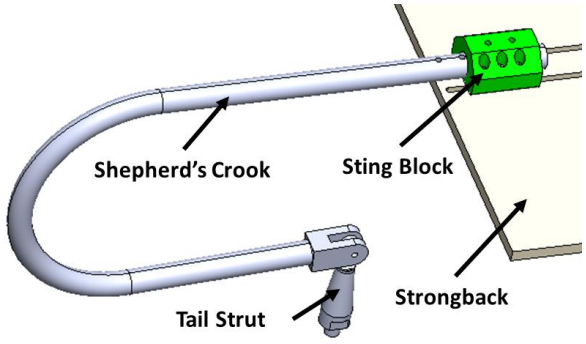

Figure 9: Tail strut assembly

The front of the strongback also attaches to the tunnel front struts, as seen in Figure 10. There are slots on the starboard and port sides of the strongback which each connect to a bracket via two 3/4-inch shoulder screws. The brackets are connected to the front struts via 1/4-inch shoulder screws. Slots are used instead of through holes so that the front struts have variable lateral placement in the 7x10, facilitating easy installation.

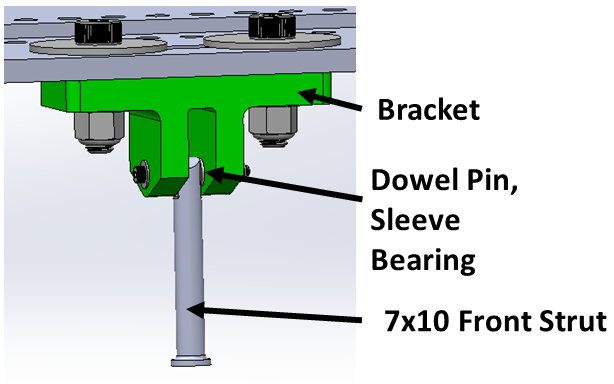

Figure 10: Front strut assembly

Just rear of the slots which attach the strongback to the front struts is a hole pattern and a large slot to mate with the rotor head stack. These 1/2-inch through holes mate with the bottom plate of the rotor head stack. These through holes have 1-inch of separation between each to vary the lateral separation of the rotors. The 55x4-inch slot shown in Figure 8 allows the rotor head stack to extend both above and below the strongback.

The diagonal slots in the strongback accommodate the tensioner/idler pulley, which maintains tension on the toothed belt regardless of the lateral location of the rotor head. The lead screw is used to adjust the tension on the pulley and the end supports are secured to the strongback via 1/2-inch socket head screws. An off-the-shelf lead screw platform nut is secured to a custom pulley bracket. The pulley bracket is secured to the strongback via 1/2-inch shoulder screws. The idler pulley is secured to the pulley bracket and provides tension to the belt. These components can be seen in Figure 11.

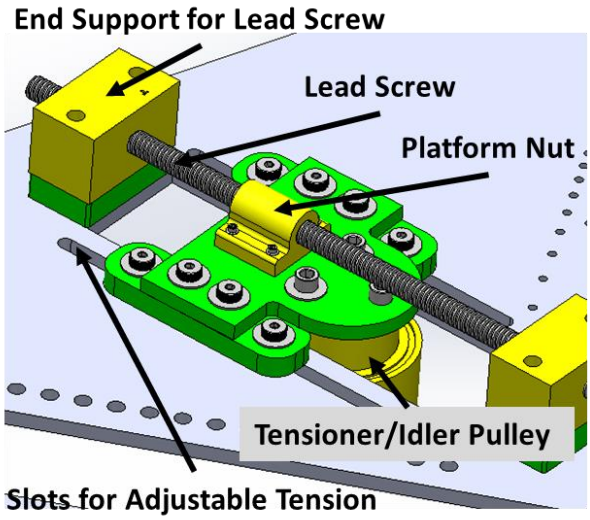

Figure 11: Tension assembly which accommodates idler pulley

As mentioned previously, the gear box attaches to the strongback via two blocks. The hole pattern on the strongback allows the gear box to be moved longitudinally as the lateral spacing of the rotor heads is varied. The hole pattern ensures that tension is seen by the belt prior to tension being applied via the idler pulley.

The accelerometer is mounted on the port side of the front of the strongback and is used to measure the pitch angle of the SBS.

The strongback also accommodates four hoist rings. The strongback itself weighs 204 pounds so the hoist rings ensure that the strong back can be transported easily via crane or forklift.

Rotor Head Stack

There are two identical rotor head stacks which hold the blades, swashplate, servos, load cell, and torque sensor, as seen in Figure 12. The rotor head stack is comprised of several plates made out of Aluminum 6061-T6, which are attached together via bolts. The rotor head and swashplate, including the blades and servos, are off-the-shelf components from the SAB Goblin 380 KSE rotor head. The plates are numbered starting at the top with plate 1. Plate 1 incorporates much of the geometry from the Goblin 380 helicopter so that the servo positions and anti-rotation piece are positioned correctly. Plates 1 and 2 are bolted together by 1/4-inch socket head cap screws, and plate 2 is fastened to the load cell. Between plates 1 and 2 there are two sets of thrust bearings and circlips so that the rotating shaft can be secured to the non-rotating plate and all of the thrust force can be transferred to plate 2 so that the force can be measured by the load cell. To attach plate 2 to the load cell, four counterbored socket head cap screws and three dowel pins are utilized.

The load cell has four internal screws that are used to mate with plate 3. Plate 3 incorporates two ball bearings which allow the center shaft to freely rotate. These can be seen in Figure 13. There are four countersunk flat head screws that mate with four standoffs, which are counterbored into plate 3. This was done for stability and accurate locating of the standoffs in plate 3. Beneath plate 3, the shaft connects to a shaft coupling which connects to the rotary torque sensor. To prevent rotation of the torque sensor, two anti-rotation brackets are installed on the standoffs. Below the torque sensor is another flex coupling which connects to a 12 mm shaft. The 12 mm shaft passes through plate 4 via an angular contact bearing. The standoffs also are counterbored into plate 4. Plate 4 connects to the strongback and can be moved laterally along the strongback to vary the spacing between the rotors. The 12 mm shaft is connected to the pulley, which

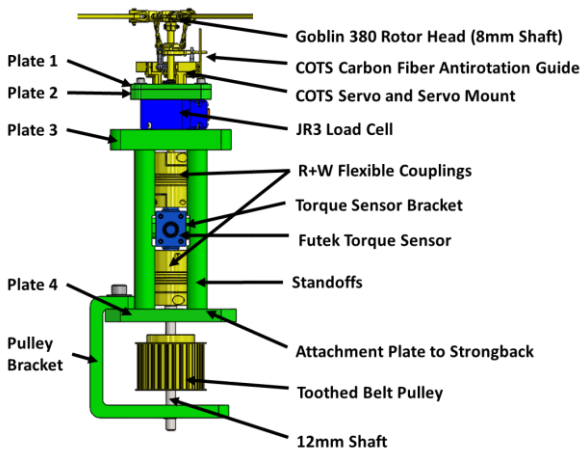

Figure 12: Rotor head stack with components highlighted

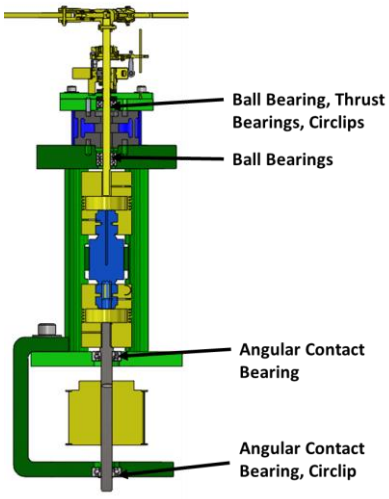

Figure 13: Cross-section view of SBS

connects to the toothed belt. The toothed belt drives the rotation of the shaft and thus the rotor. There is a pulley bracket which holds the 12 mm shaft in place and ensures minimal deflection due to the tension force on the belt.

The lateral spacing between the rotors can be changed at a resolution of 1 inch, as this is the spacing between the through holes on the strongback and plate 4.

The distance from the top face of the strongback to the top of the rotor head is approximately 15.4 inches. This height was mainly driven by the dimensions of the flex coupling and rotary torque sensor. The pulley bracket also extends 4.25 inches below the top face of the strongback. Additional dimensions can be seen in Figure 14.

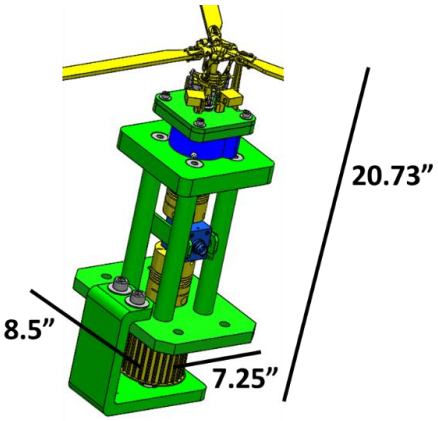

Figure 14: Overall dimensions of rotor head stack

LOADS AND STRESS ANALYSIS

A structural analysis was conducted for each component of the SBS to ensure that the components had sufficient safety factors for the planned testing configurations. The structural analysis consisted of hand calculations as well as Finite Elements Analysis (FEA). Dassault Systèmes computer aided design (CAD) software package, SolidWorks, was used to generate the CAD model, the drawings, and was used to conduct the FEA.

The loads used for the calculations come from the maximum expected loads that will be encountered during experimental testing. The maximum loads used for calculations were 50 lb of thrust per rotor, 240 in-lb of torque per rotor, 60 lb of in-plane force per rotor, 500 in-lb of motor torque, 270 lb of belt force, and 92 lb of gear force. Belt force and gear force were derived from the geometry of the belt, gear, and the operating conditions. The locations of the forces and moments experienced by the SBS are sketched in Figure 15.

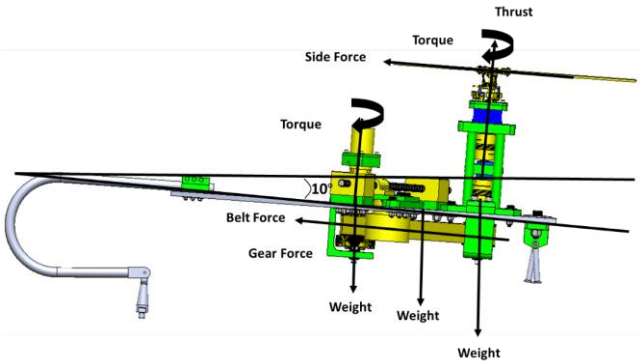

Figure 15: Free body diagram of SBS at maximum nose down pitch

Finite Element Analysis

The SolidWorks FEA solver was used to conduct structural analysis of each component of the SBS to determine maximum stresses and maximum deflection. Each study was conducted on an individual part of the SBS assembly. The constraints that were applied in SolidWorks were intended to mimic the physical constraints of the assembly. It was assumed that all forces would directly propagate to each sequential component, which is a conservative assumption. Loads were applied to the surfaces which would transfer the forces in each component. Maximum stresses and safety factors are listed in Table 1. For each FEA study, the mesh was refined, and a convergence study was conducted to ensure that the stress converged. In some cases, stress singularities appeared. Stress singularities occur when, despite mesh refinement, the stress does not converge to a specific value. Instead, the stress continues to increase, theoretically to infinity. If the stress singularity occurred in a

critical location on the part, the geometry of the part was smoothed, for example by adding a fillet. However, if the stress singularity occurred at a location that was not critical (for example on the inside of a counterbore where a screw is inserted), the mesh was refined to ensure that the part had no critical stresses elsewhere and the singularity was ignored.

Load and Stress Calculations for Hardware

Shear and tensile forces for each screw and dowel pin in the assembly were calculated to ensure that the off-the-shelf components would still maintain a sufficient safety factor under testing conditions.

After calculating the tensile (equation 1) and shear stresses (equation 2), the Von Mises stress was calculated (equation 3). The shear stress was calculated both from the shear force and the force which resulted from bending moments. As a worst-case scenario, it was assumed that these forces acted in the same direction. To obtain safety factors, the ultimate strength of the material was divided by the Von Mises stress [22].

Equation 1 $$\sigma_{tensile} = \frac{F_{tensile}}{A_{tensile}}$$

Equation 2 $$\tau_{shear} = \frac{4F_{shear}}{3A_{shear}}$$

Equation 3 $$\sigma_{Von\ Mises} = \sqrt{\sigma_{tensile}^2 + 3\tau_{shear}^2}$$

Similar calculations were conducted for the off-the-shelf bearings to ensure that the bearings would maintain a minimum safety factor.

RESULTS

To perform testing in the 7x10 wind tunnel, a safety factor of 4 on ultimate strength and 3 on yield strength is required [23]. The SBS was designed to meet and exceed such required safety factors, as seen in the list of safety factors laid out in Tables 1 and 2. Further, because the SBS mechanical design incorporates safety factors far beyond 5 on yield strength, a fatigue analysis was not required [22].

CONCLUSIONS

A new test bed capability was designed, analyzed, and as of December 2020 is in the manufacturing process. The loads and stress analysis show that the SBS will maintain and exceed the required safety factors for all operating conditions. The purpose of this test bed is to test the Urban Air Mobility Side-by-Side concept vehicle. The SBS test bed allows for lateral adjustment of the rotors and also allows for nose up and nose down pitching. The main experimental goal for this test bed is to take rotor performance measurements for various degrees of rotor overlap to experimentally determine the optimal rotor overlap. The SBS will enter the U.S. Army's 7-by-10 Foot Wind Tunnel for an initial test campaign and will have following test entries as well. Ultimately, the experimental testing of the SBS will support technological growth for the advancement of the emerging Urban Air Mobility market and will contribute to NASA's growing suite of reference vehicles with computational and experimental data available in the public domain.

Author contact: Haley Cummings
haley.cummings@nasa.gov

ACKNOWLEDGMENTS

This work was funded by NASA's Revolutionary Vertical Lift Technology Project.

The authors would like to acknowledge the NASA machine shop team led by Robert Kornienko and Vincent Derilo for their continued guidance and excellence in machining. Thanks also to the 7x10 Wind Tunnel team including Gary Fayaud, Samuel Huang, Stephen Nance, Henry Schwoob, and William Peneff. Enrico Bernabei from SAB is also appreciated for his contributions and assistance. Thanks to Farid Haddad and Alex Sheikman for always sharing knowledge and experience. Thanks to Sarah Conley and Geoffrey Ament for your support in the design of the SBS. Thank you to Michelle Dominguez for reviewing the paper. Thank you to Natalia Perez Perez for always having great suggestions and for your continued support. Finally, thank you to Dr. William Warmbrodt for the constant support and leadership.

REFERENCES

[1] Johnson, W., Silva, C., and Solis, E., 2018, "Concept Vehicles for VTOL Air Taxi Operations," *AHS Technical Conference on Aeromechanics Design for Transformative Vertical Flight*, AHS International, San Francisco, California.

[2] Russell, C., Jung, J., Willink, G., and Glasner, B., 2016, "Wind Tunnel and Hover Performance Test Results for Multicopter UAS Vehicles," *72nd Annual Forum*, American Helicopter Society, West Palm Beach, Florida.

[3] Russell, C. R., and Sekula, M. K., 2017, "Comprehensive Analysis Modeling of Small-Scale UAS Rotors," *AHS International 73rd Annual Forum & Technology Display*, AHS International, Fort Worth, Texas.

[4] Russell, C., Willink, G., Theodore, C., Jung, J., and Glasner, B., 2018, *Wind Tunnel and Hover Performance Test Results for Multicopter UAS Vehicles*, NASA/TM-2018-219758, Moffett Field, California.

[5] Conley, S., and Russell, C., 2020, "Mechanical

Design of the Multirotor Test Bed," *Aeromechanics for Advanced Vertical Flight Technical Meeting*, Vertical Flight Society, San Jose, California.

[6] Russell, C., and Conley, S., 2020, "The Multirotor Test Bed-A New NASA Test Capability for Advanced VTOL Rotorcraft Configurations," *76th Annual Forum & Technology Display*, Vertical Flight Society, Virginia Beach, Virginia.

[7] Conley, S., Russell, C., Kallstrom, K., Koning, W., and Romander, E., 2020, "Comparing RotCFD Predictions of the Multirotor Test Bed with Experimental Results," *76th Annual Forum & Technology Display*, Vertical Flight Society, Virginia Beach, Virginia.

[8] Silva, C., Johnson, W., Antcliff, K. R., and Patterson, M. D., 2018, "VTOL Urban Air Mobility Concept Vehicles for Technology Development," *2018 Aviation Technology, Integration, and Operations Conference*, AIAA, Dallas, Texas.

[9] Silva, C., and Johnson, W., 2018, "Multidisciplinary Conceptual Design for Reduced-Emission Rotorcraft," *Specialists Conference on Aeromechanics Design for Transformative Vertical Flight*, AHS International, San Francisco, California.

[10] Johnson, W., and Silva, C., 2018, "Observations from Exploration of VTOL Urban Air Mobility Designs," *7th Asian/Australian Rotorcraft Forum*, Vertical Flight Society, Jeju Island, Korea.

[11] Ventura Diaz, P., and Yoon, S., 2018, "High-Fidelity Computational Aerodynamics of Multi-Rotor Unmanned Aerial Vehicles," *AIAA Aerospace Sciences Meeting, 2018*, American Institute of Aeronautics and Astronautics Inc, AIAA, Kissimmee, Florida.

[12] Johnson, W., 2020, "A Quiet Helicopter for Air Taxi Operations," *Aeromechanics for Advanced Vertical Flight Technical Meeting*, Vertical Flight Society, San Jose, California.

[13] Tishchenko, M. N., 1997, "Mil Design Bureau Heavy-Lift Helicopters," J. Am. Helicopter Soc., **42**(2), pp. 137–148.

[14] Mil, M. L., 1967, *Helicopters: Calculation and Design, Volume I*, NASA TTF-494.

[15] Johnson, W., 2013, *Rotorcraft Aeromechanics*, Cambridge University Press, New York, New York.

[16] Silva, C., 2016, "Conceptual Design of a Remote Controlled Electric Powered Helicopter for World Record Distance, Endurance, and Climb," *Technical Meeting on Aeromechanics Design for Vertical Lift*, American Helicopter Society, San Francisco, California.

[17] Ventura Diaz, P., Johnson, W., Ahmad, J., and Yoon, S., 2019, "Computational Study of the Side-by-Side Urban Air Taxi Concept," *Vertical Flight Society's 75th Annual Forum*, VFS International, Philadelphia, Pennsylvania.

[18] Korotkevich, M. M., Midzyanovskiy, S., and Ivchin, V., 2014, "Highspeed Rotorcraft of the MI-450 Family New Generation of Cross-Arrangement Rotary-Wing Aircraft," *40th European Rotorcraft Forum*, American Helicopter Society, Southampton, United Kingdom.

[19] Diaz, P. V., Johnson, W., Ahmad, J., and Yoon, S., 2019, "The Side-by-Side Urban Air Taxi Concept," *Aviation Forum*, American Institute of Aeronautics and Astronautics, Dallas, Texas.

[20] Barrett, R. T., 1990, *Fastener Design Manual*, NASA Reference Publication 1228, Cleveland, Ohio.

[21] Oberg, E., Jones, F. D., Horton, H. L., and Ryffel, H. H., 2012, *Machinery's Handbook*, Industrial Press, New York, New York.

[22] Budynas, R. G., and Nisbett, J. K., 2011, *Shigley's Mechanical Engineering Design*, McGraw-Hill, New York, New York.

[23] *National Full-Scale Aerodynamics Complex Operations Manual: Part III; Test Planning Guide for Investigations in 40- by and 80- by 120-Foot Wind Tunnel Facility*, 1993, NFAC Staff, Moffett Field, California.

Table 1: List of safety factors from FEA

Part	Material	Max Stress (psi)	Yield Strength (psi)	SF Yield
Servo Support to Load Cell	Al 6061	2578	35000	13.58
Head to Load Cell	Al 6061	3956	35000	8.85
Below Load Cell	Al 6061	3533	35000	9.91
Standoffs	17-4	7201	118000	16.39
Pulley Bracket	17-4	5139	185000	36.00
Stack to Strongback	Al 6061	530	35000	66.03
Shaft (12mm)	440C	31870	275000	8.63
GB Housing	17-4	10970	185000	16.86
GB Support	17-4	13260	185000	13.95
GB to SB Block	17-4	837	185000	221.00
Plate 5 (Top GB Adapter)	Al 6061	2683	35000	13.05
Plate 6 (Bottom GB Adapter)	Al 6061	2883	35000	12.14
Shaft (15 mm - Motor Side)	440C	17310	275000	15.89
Shaft (15 mm - Opposite Side)	440C	26110	275000	10.53
Tensioner Pulley Bracket 1	17-4	1184	185000	156.25
Tensioner Pulley Bracket 2	17-4	458	185000	404.02
Lead Screw Support Block	17-4	425	185000	435.81
Strongback	17-4	20650	185000	8.96
Front Strut Clevis	17-4	1754	185000	105.47

*GB = Gear Box

Table 2: List of fastener safety factors

Fastener	Location	Max Stress (psi)	SF Ultimate
1/4-28 SHCS	Plates 1 & 2	3085.00	45.38
M6 SHCS	Plate 2	568.70	246.18
1/2-20 Flat Head	Plates 3 & 4	78.17	1790.97
1/2" Shoulder 3/8-16 thread	Plate 4	413.00	338.98
1/2-20 SHCS	Pulley Bracket	3223.00	43.44
1/4-28 SHCS	Plate 5 Top GB Adapter	5433.00	25.77
M5 SHCS	Plate 6 Bottom GB Adapter	16882.00	8.29
M5 SHCS	Neugart to GB	14366.00	9.75
1/2" Shoulder 3/8-16 thread	GB Plate to GB	2158.90	64.85
1/2-20 SHCS	GB Plate to SB Block	78.17	1790.97
1/4" Shoulder 10-24 thread	Block to SB	5164.73	27.11
1/2" Shoulder 3/8-16 thread	Idler Bracket 1	793.90	176.34
1/2" Shoulder 3/8-16 thread	Idler Bracket 2	793.90	176.34
M12x1.75 SHCS	Idler Pulley	3516.85	39.81
#8-36	Lead Screw Platform Nut	12131.00	11.54
1/2" Shoulder 3/8-16 thread	Lead Screw End Support	793.90	176.34
3/4" Shoulder 5/8-11 thread	Front Struts	350.10	399.89
1/4" Shoulder 10-24 thread	Rear Strut Connection	2945.60	47.53

*GB = Gear Box

**all screws are made from black oxide alloy steel and have an ultimate strength of 140,000 psi